TWENTYFITH EUROPEAN ROTORCRAFT FORUM

Paper n° G4

ON THE IMPORTANCE AND EFFICIENCY OF 2/REV IBC FOR NOISE, VIBRATION AND PITCH LINK LOAD REDUCTION

BY

M. MÜLLER
U.T.P. ARNOLD
D. MORBITZER
ZF LUFTFAHRTTECHNIK GMBH, GERMANY

SEPTEMBER 14-16, 1999
R O M E
ITALY

ASSOCIAZIONE INDUSTRIE PER L'AEROSPAZIO, I SISTEMI E LA DIFESA
ASSOCIAZIONE ITALIANA DI AERONAUTICA ED ASTRONAUTICA

ON THE IMPORTANCE AND EFFECTIVENESS OF 2/REV IBC FOR NOISE, VIBRATION AND PITCH LINK LOAD REDUCTION

M. Müller
U.T.P. Arnold
D. Morbitzer

ZF Luftfahrttechnik GmbH, Germany

1. Abstract

This paper presents experimental and theoretical results that help to assess the importance and effectiveness of 2/rev IBC/HHC active rotor control. Wind tunnel and flight test results will be shown which clearly indicate the positive impact of the second rotor harmonic frequency for vibration reduction. Simple models will be used to explain two physical mechanisms of inter-harmonic coupling that are believed to be predominant in causing the 2/rev effects discussed in this paper. Beside the usefulness in reducing vibrations, 2/rev has also proven to be essential to reduce BVI noise and pitch link loads. Selected experimental results are presented to show the effectiveness with respect to these optimization goals.

2. Notation

A_n	deg	IBC/HHC control amplitude of n/rev harmonic component
a/R		relative (equivalent) hinge offset
$C_{(...)} = (...) / (\pi\rho R^4 \Omega^2 [R])$		thrust, moment coefficient
$I_\beta = \int r^2 dm$	kgm^2	blade flap momentum of inertia
M_x, M_y	Nm	rotor roll, pitch moments
N		number of blades
n		order of harmonic component
R	m	rotor radius
$\underline{S}$		IBC to vibration response transfer matrix (non-linear, steady-state)
$S_\beta = \int r dm$	kgm	blade static flap mass Momentum
T	N	rotor thrust
$\underline{T}$	N[m]/ rad	IBC to vibration response transfer matrix (linear, steady-state)
$\underline{u}$	rad	vector of higher harmonic control inputs (sin, cos compon.)
Z_s	N	blade root vertical shear force
$\underline{z}$	N[m]	vector of vibration components (sine, cosine components.)
β	deg, rad	flap angle
$\gamma = (\rho C_{l\alpha} c R^4) / I_\beta$		LOCK number
$\delta = (w_{Ro} - w_i) / (\Omega R)$	- , rad	inflow ratio/angle
$\underline{\vartheta}_{HHC}$	rad	vector of higher harmonic control inputs (sin, cos compon.)
ϑ_{twist}	rad	built-in blade twist
ϑ_{root}	deg, rad	blade pitch angle at blade root
$\mu = u_{Ro} / (\Omega R)$		advance ratio
ρ	kg/m^3	air density
$\sigma = cN / (\pi R)$		blade solidity
φ_n	deg	IBC/HHC control phase angle of n/rev harmonic component
ψ	deg	rotor azimuth angle (=non-dimensional time)
Ω	rad/s	rotor rotational speed
$(...)' = d(...) / d\psi$		first derivative with respect to rotor azimuth

3. Introduction

Active Rotor Control by blade root actuation has proven highly valuable and successful in reducing several negative effects associated with helicopter rotors operating in tangential flow. At high forward speed various problems arise due to the asymmetric flow condition, high MACH numbers, the large wake skew angle and the requirement to satisfy momentum trim. Figure 1 gives an symbolic overview of the more important ones of these effects.

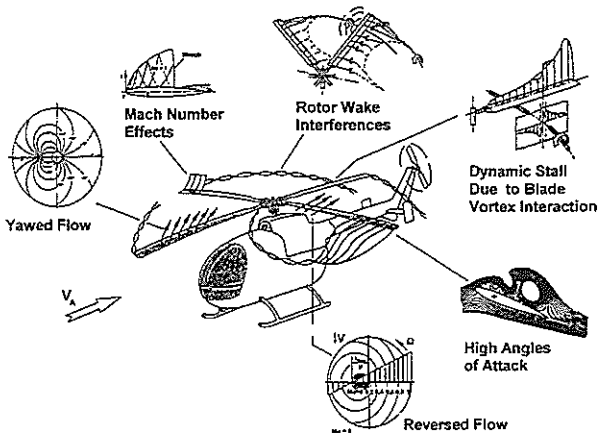

Figure 1: Negative Effects Associated with Helicopter Rotors in Tangential Flow

Two technical approaches of higher harmonic blade root pitch control have been developed and tested in the past, both competing with respect to the required effort and the gained benefit.

Company	ZFL			DLR	McDonnell Douglas	Sikorsky	Aerospatiale	Boeing Vertol	
Campaign	Flight Test	Wind Tunnel Test (NASA Ames)	Flight Test	Wind Tunnel Test (DNW)	Flight Test	Flight Test	Flight Test	Wind Tunnel Test	
Test Bed	BO105	1:1 BO105 Rotor	BO105	40% BO105 Model Rotor	OH-6A	S-76	SA-349	Model 179	1:6 CH-47D Model Rotor
Year	1990/91	1993/94	1998	1990	1982	1985	1985	1981	1985
Control Concept	IBC OL	IBC OL	IBC OL	HHC OL	HHC OL/CL	HHC OL	HHC OL/CL	HHC OL/CL	HHC CL
Control Parameter	3Ω 4Ω 5Ω +/- 0.16° +/- 0.40°	2Ω 3Ω 4Ω 5Ω 6Ω Max. +/- 2°	2Ω 3Ω 4Ω 5Ω 6Ω +/- 1.1°	3Ω 4Ω 5Ω +/- 0.8 +/- 1.2	3Ω 4Ω 5Ω +/- 2.00° +/- 0.33°	3Ω 4Ω 5Ω +/- 1°	2Ω 3Ω 4Ω +/- 1.0° +/- 0.8°	3Ω 4Ω 5Ω +/- 1.3°	2Ω 3Ω 4Ω +/- 3°
Advance Ratio μ	0.15 0.26	0.10 0.15 0.30 0.40 0.45	0.10 0.15	0.10 0.15 0.20 0.35	0.10 : 0.24	0.07 : 0.25	0.12 0.31	0.10 0.30	0.4
Noise Reduction	✓	max. 8dB	max. 6dB	max. 6dB			max. 6dB		
Vibration Reduction	50%-80%	max. 85%	50%-80%	30%	60%-70%	40%-60%	80%	90%	✓
Performance Improvement		max. 7%			NO	NO	✓	1,7% - 4%	✓
Load Reduction		✓							
Structural Blade Load	↗	↗ ↘			↗			↗	
Pitch Link Load		↗			↗			↗	
Critical Loads		NO			NO			NO	NO
References				[2], [3]	[4], [5]	[6]	[7]	[8], [9]	[10]

Figure 2: *Overview of Experimental Research Activities and their Results in the Field of HHC (Higher Harmonic Control) and IBC(Individual Blade Control)*

One system, commonly called HHC (Higer Harmonic Control), enables higher frequency motions of the swashplate to produce additional harmonic blade pitch variations. As result of the kinematic properties these systems are restricted to particular multiples of the rotor frequency, namely kN-1, kN and kN+1 for k=1,2,3...

The other system, denoted as IBC (Individual Blade Control), allows to control each blade individually without any restriction of the applied frequencies. Beside the deviations in the technical lay-out, the main difference is the possibility of the IBC-type systems to introduce 2/rev control in modern rotors having more than three blades. Figure 2 gives an overview over various experimental activities that were focused on the application of HHC or IBC. Since the majority of the test campaigns had to cope with the restrictions of HHC the question, how useful 2/rev control might be, did not actually arise. For details of IBC systems as designed and used by ZFL for several wind tunnel and flight test campaigns see Refs. [13], [16], [17] and [18].

Nevertheless, the value of 2/rev at least for reducing rotor power required is widely accepted. This particular application seems to have triggered the general interest in HHC as can be derived from early publications like Ref. [19]. The necessity of 2/rev for vibration reduction, however, is frequently questioned. The obvious properties of the transformation between rotating and the non-rotating frame are believed to imply that 2/rev has to be much less effective than (N-1)/rev, N/rev and (N+1)/rev inputs. As a matter of fact, even such sophisticated programs as CAMRAD clearly underpredict the 2/rev effect compared to wind tunnel and flight test results. By using the experimental IBC systems designed, manufactured and operated by ZFL it was possible for the first time to extensively investigate those 2/rev effects.

In the following sections the focus is solely put on the 2/rev results. For comparison with the proven effects of the HHC frequencies and for a comprehensive description of the test results gained with ZFL's IBC systems see Refs. [12], [13] and [15].

4. Noise Reduction through 2/rev IBC

One main application of higher harmonic blade pitch control is to reduce the BVI noise radiation. Therefore, ZFL, having participated in several national and international research programs, has conducted intensive experimental investigations of noise reduction through IBC. The 1993/94 full-scale wind tunnel tests at the NASA Ames research center led to promising results in this field, Ref. [18]. The RACT flight tests carried out last year were used to validate these impressive results. For noise measurements in the wind tunnel, the rotor operation condition was adjusted to a high BVI condition as usually encountered during landing approach. Therefore, the same flight conditions were investigated during the RACT flight tests. The ground based measurement hardware consisted of 3 microphones, one on

the advancing, one on the retreating side and the third one on the center line of the flight path, all of them located according to the ICAO regulations.

Figure 3 shows the maximum A-weighted sound pressure level L_{Amax} versus the single-harmonic 2/rev blade pitch control phase angle φ_2. Maximum noise reduction of more than 5dB was achieved at $\varphi_2 \approx 60$deg near the optimum phase angle expected according to the wind tunnel results, Ref. [12]. Given this considerable effect of 2/rev control on rotor noise it is of great interest what effect the same control inputs exhibit on the vibrations in the non-rotating frame. Former HHC results, Ref. [23], for the same type of rotor had shown that noise and vibration reduction could never be achieved simultaneously when using the HHC frequencies 3/rev, 4/rev and 5/rev. For details on the comparison between wind tunnel and flight test results see Ref. [12].

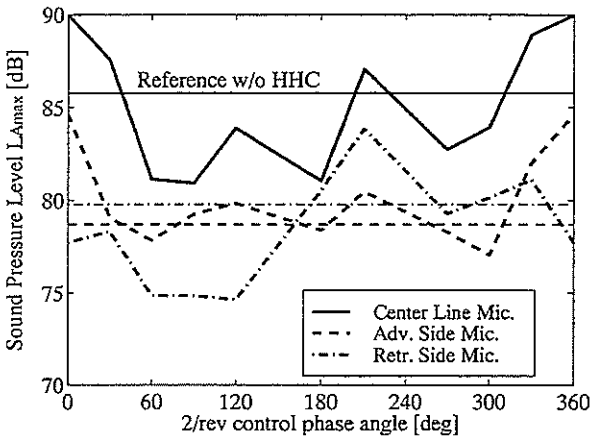

Figure 3: Rotor Sound Pressure Levels vs. IBC Phase Angle for Single-Harmonic 2/rev Control, A_2 = 1deg (RACT flight test results, BO-105S1, μ = 0.15, γ = -6deg)

5. Vibration Reduction through 2/rev IBC

The rotor induced vibrations of a helicopter originate from the unsteady aerodynamic forces acting on the rotor blades. They are caused by phenomena which can in many cases be associated with fixed rotor azimuth positions (see Figure 1). The resulting aerodynamic loads are of periodical type with the corresponding frequency spectra mainly consisting of so-called rotor harmonics $n\Omega$. They excite the rotor blades to oscillations in both flapwise and lead-lag direction. These blade motions combined with inertial and elastic forces finally determine the blade root loads. To obtain the resulting vibrations in the fixed frame the forces and moments of all blades have to be added and transformed into the non-rotating system. Due to this transformation several harmonics cancel each other and the resulting vibrations in the fixed frame only consist of frequencies which are integral multiples of the blade passage frequency $kN\Omega$ with k = 1,2,3... Out of these harmonic components, the lowest one is not only associated with highest amplitude but furthermore represents the most straining one for the passengers.

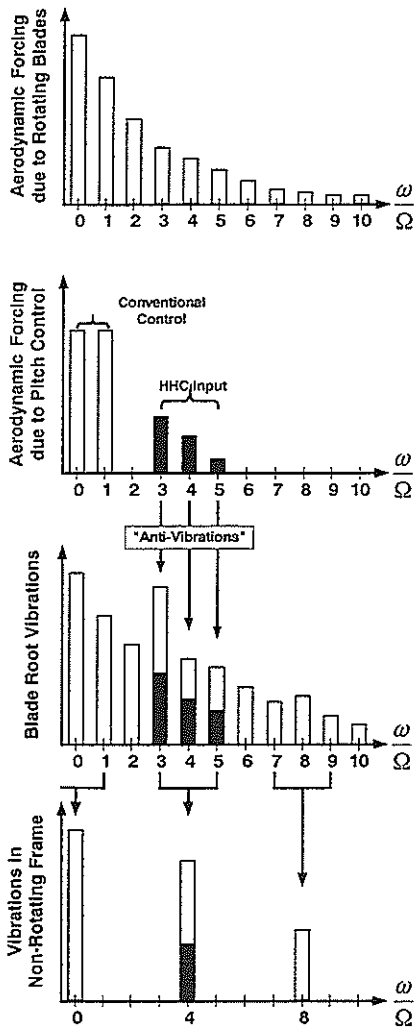

Figure 4: Transformation of Vibratory Loads from the Rotating into the Non-Rotating Frame and Application of HHC to Reduce Vibrations (4-Bladed Rotor)

It is caused by blade load components of the frequencies (N-1)/rev, N/rev and (N+1)/rev in the rotating frame, see Ref. [26]. These harmonics can be affected by controlled blade pitch changes of the same frequencies. With properly adjusted amplitudes and phases the blade oscillations can be controlled in a way that leads to a reduction of the resulting hub loads and subsequently to the desired minimization of the fuselage vibrations, see Figure 4.

Because of this correlation between blade loads in the rotating frame, vibrations in the non-rotating frame and the corresponding higher harmonic blade pitch control inputs, mostly (N-1)/rev, N/rev and (N+1)/rev control as can be provided by HHC systems has been considered for vibration reduction. Consequently, 2/rev control was not believed to be of great relevance for rotors with more than four blades, since blade pitch inputs with this frequency do not have the same direct feedthrough to vibrations in the fixed frame.

5.1 Experimental Results

Although the validation of the wind tunnel test results with respect to noise reduction was the main purpose of

the RACT flight tests, accelerations in the fuselage were measured and recorded, too. The highly sophisticated data acquisition system installed in the BO-105S1 (Ref. [13]) provided acceleration signals in three axis at the top of the main gear box, at the co-pilot seat and in the payload compartment. These vibration data have facilitated the extensive evaluation of the effect of 2/rev control on vibrations, compare Refs. [12] and [13].

5.1.1 Mathematical Description of IBC Transfer Behavior and Effectiveness Measure

Earlier evaluations of the helicopter vibrations had used measured 4/rev hub vibrations in the non-rotating frame, which were then analyzed in the sine/cosine plane. This method leads to the well-known ellipses that describe the linear, quasi-steady transfer behavior between the IBC inputs and the resulting vibrations. The model relates the cosine and sine components of the higher harmonic pitch control angles arranged in the vector $\underline{\vartheta}$ to the cosine and sine components of the 4/rev vibrations in the fuselage arranged in the vector $\underline{z}$ and can be written as the following linear transformation.

$$\underline{z} = \underline{\underline{T}}\,\underline{\vartheta}_{HHC} + \underline{z}_0$$

Such a model seemed to be appropriate for linear time-periodic systems. The shape and size of the ellipse depends on the $\underline{\underline{T}}$-matrix elements, see Ref. [12] for details. This linear mapping of the input $\underline{\vartheta}_{HHC}$ to the output $\underline{z}$ is well suited to describe the transfer behavior between 3/rev, 4/rev, and 5/rev inputs and the 4/rev vibratory response. For 2/rev inputs, however, this linear mapping does not provide an accurate representation of the transfer behavior to the measured 4/rev fuselage vibrations. Therefore the linear formulation has been extended by a quadratic term to

$$\underline{z} = \underline{\underline{T}}\,\underline{u} + diag(\underline{u})\,\underline{\underline{S}}\,\underline{u} + \underline{z}_0 ,$$

where the cosine and sine components of the 2/rev input now form the vector $\underline{u}$. It can be shown that this non-linear transformation represents the system behavior much better and provides an astonishing well suited means of interpolation for the measured data. The determination of the two transfer matrices is based on the least-mean square method. For a given number of measurements it yields the following set of equations.

$$\underbrace{\begin{bmatrix} \Sigma u_{1i}^2 & \Sigma u_{1i}u_{2i} & \Sigma u_{1i}^3 & \Sigma u_{1i}^2u_{2i} & \Sigma u_{1i} \\ \Sigma u_{1i}u_{2i} & \Sigma u_{2i}^2 & \Sigma u_{1i}^2u_{2i} & \Sigma u_{1i}u_{2i}^2 & \Sigma u_{2i} \\ \Sigma u_{1i}^3 & \Sigma u_{1i}^2u_{2i} & \Sigma u_{1i}^4 & \Sigma u_{1i}^3u_{2i} & \Sigma u_{1i}^2 \\ \Sigma u_{1i}^2u_{2i} & \Sigma u_{1i}u_{2i}^2 & \Sigma u_{1i}^3u_{2i} & \Sigma u_{1i}^2u_{2i}^2 & \Sigma u_{1i}u_{2i} \\ \Sigma u_{1i} & \Sigma u_{2i} & \Sigma u_{1i}^2 & \Sigma u_{1i}u_{2i} & \Sigma i \end{bmatrix}}_{\underline{\underline{A}}} \cdot \underbrace{\begin{bmatrix} s_{11} \\ s_{12} \\ t_{11} \\ t_{12} \\ z_{01} \end{bmatrix}}_{\underline{t}_1} = \underbrace{\begin{bmatrix} \Sigma z_{1i}u_{1i} \\ \Sigma z_{1i}u_{2i} \\ \Sigma z_{1i}u_{1i}^2 \\ \Sigma z_{1i}u_{1i}u_{2i} \\ \Sigma z_{1i} \end{bmatrix}}_{\underline{y}}$$

This can be solved by extending the input vector as follows.

$$\underline{u}_i^{\cdot} = \begin{bmatrix} u_{1i} & u_{2i} & u_{1i}^2 & u_{1i}u_{2i} & 1 \end{bmatrix}^T$$

With $\underline{\underline{A}} = \left(\underline{\underline{U}}^*\right)^T \underline{\underline{U}}^*$ and $\underline{y} = \left(\underline{\underline{U}}^*\right)^T \underline{z}^*$ the first column $\underline{t}_1$ of the non-linear mapping is given by

$$\underline{t}_1 = [s_{11} \quad s_{12} \quad t_{11} \quad t_{12} \quad z_{01}]^T = \left(\left(\underline{\underline{U}}^*\right)^T \underline{\underline{U}}^*\right)^{-1} \left(\underline{\underline{U}}^*\right)^T \underline{z}^* .$$

In the same manner the second column of the transfer matrix can be computed, where the related second input vector is now described by

$$\underline{u}_i^{\cdot} = [u_{1i} \quad u_{2i} \quad u_{1i}u_{2i} \quad u_{2i}^2 \quad 1]^T .$$

For quantitatively assessing the effect of different IBC frequencies on the vibrations a simple numerical measure was defined. The effectiveness for linear transfer behavior is given in [12] and is defined as the ratio of resultant vibration level to HHC input amplitudes. The mean vibratory response magnitude can be approximated by the radius E of a circle having the same area as the actual ellipse described by the T-matrix components. For the non-linear transformation which is applied to the transfer behavior between 2/rev control and 4/rev vibrations this method is no longer applicable, because this mapping does not have a finite area. Therefore, the effectiveness is now defined as the distance of the measurements in the sine/cosine-plane from the reference data point for unity excitations of 1deg. For k measurements the over-all HHC effectiveness is defined by

$$E = \frac{1}{k}\sum_{i=1}^{k} \left|\underline{Z}_i - \underline{Z}_0\right| .$$

One should note that this equation coincides with the former definition when applied to a linear system that shows a perfect circle in the cosine/sine-plane. All wind tunnel and flight test data presented in the following sections have been analyzed with this non-linear transformation method.

5.1.2 Flight Tests

The measured accelerations at the co-pilot seat are shown in Figure 5. The magnitude of the 4/rev accelerations versus the 2/rev IBC phase angle as well as the components in the cosine/sine-plane are plotted. In addition, the figure presents the interpolation that results from the non-linear mapping. As can be seen, the 2/rev input is able to reduce the vibrations by more than 60%. The identified transformation matches the measured data very well, which proves the suitability of the non-linear formulation.

In contrast to former HHC results, where noise and vibration reduction were never achieved simultaneously, Ref. [23], the evaluation of the 2/rev control data shows decreased vibration and noise levels for almost the same phase angle (Figure 3). The previously mentioned idea of vibration reduction by superposing "anti"-vibrations intentionally generated through HHC of the same frequency does not cover this effect of simultaneous noise and vibration reduction through 2/rev control. Consequently, the influence of 2/rev has to be based on another mechanism.

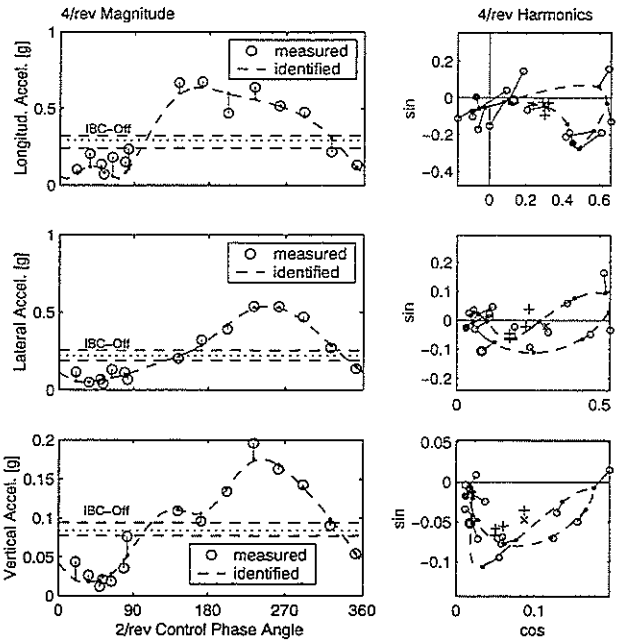

Figure 5: Accelerations at Co-Pilot Seat vs. IBC Phase Angle for Single Harmonic 2/rev Control, A_2 = 1deg (RACT Flight Test Results, BO-105S1, μ = 0.15, γ = -6deg)

5.1.3 Wind Tunnel Tests

The vibration results of the wind tunnel tests are presented in Figure 6 and Figure 7. The magnitudes of the 4/rev hub loads versus the IBC phase angle and the corresponding components in the cosine/sine-plane are plotted for two flight conditions.

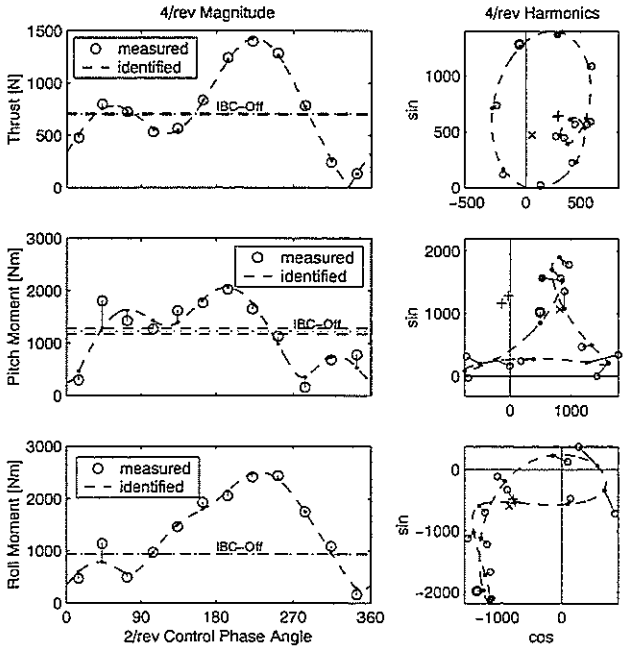

Figure 6: 4/rev Thrust, Roll and Pitch Moment at Rotor Hub (Non-Rotating Frame) vs. IBC Phase Angle for Single-Harmonic 2/rev Control, A_2 = 1deg (Wind Tunnel Data, Full-Scale BO-105 Rotor, μ = 0.15, α_{Ro} = 2,9deg)

Again, the figures contain the interpolation results from the identified transfer matrices and confirm the suitability of the non-linear mapping. Similar to the flight tests, 2/rev control has an considerable effect on the vibrations. Figure 7, however, also shows that applying a single control frequency alone does not provide the means to reduce vibrations in more than one axis simultaneously. In the example presented here, the amplitude was correctly set for optimum suppression of thrust vibrations, but was too small with respect to pitch and too large with respect to roll moments.

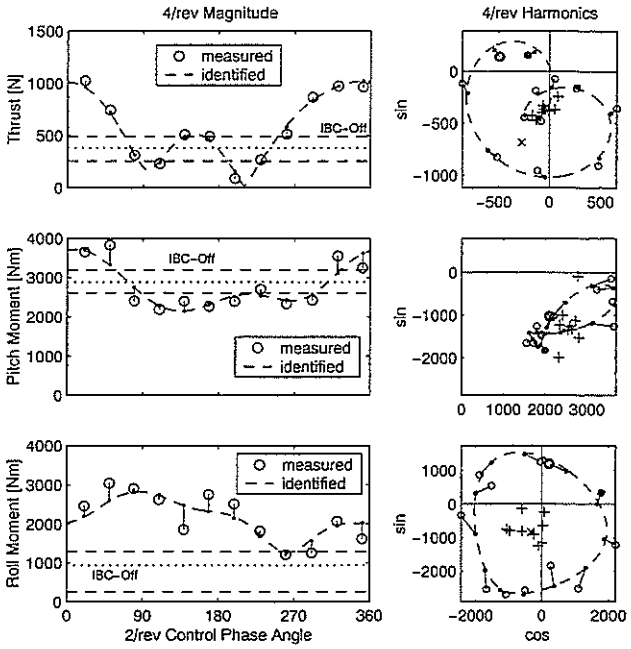

Figure 7: 4/rev Thrust, Roll and Pitch Moment at Rotor Hub (Non-Rotating Frame) vs. IBC Phase Angle for Single-Harmonic 2/rev Control, A_2 = 1deg (Wind Tunnel Data, Full-Scale BO-105 Rotor, μ = 0.4, α_{Ro} = -9deg)

5.1.4 Effectiveness Identified from Wind Tunnel Test Data

Figure 8 summarizes the wind tunnel evaluation concerning the IBC effect on vibratory loads. For all tested higher harmonic inputs Figure 8 presents the resulting effectiveness on thrust, pitch and roll moments based on 1deg higher harmonic blade pitch inputs. Although the effectiveness of 2/rev turns out to be smaller than it is for the other frequencies, 2/rev is still a valuable frequency. One has to keep in mind that (servo-) hydraulic IBC systems as they were used for the presented experiments are limited to a certain maximum travel velocity. This limit yields a hyperbolic characteristic of available control amplitudes over the control frequency, where 2/rev allows by far the highest amplitudes. As a matter of fact, the available 4/rev amplitude only reaches approximately 50% of the corresponding 2/rev authority. Thus, the lower effectiveness of 2/rev is compensated by the availability of higher amplitudes at this frequency.

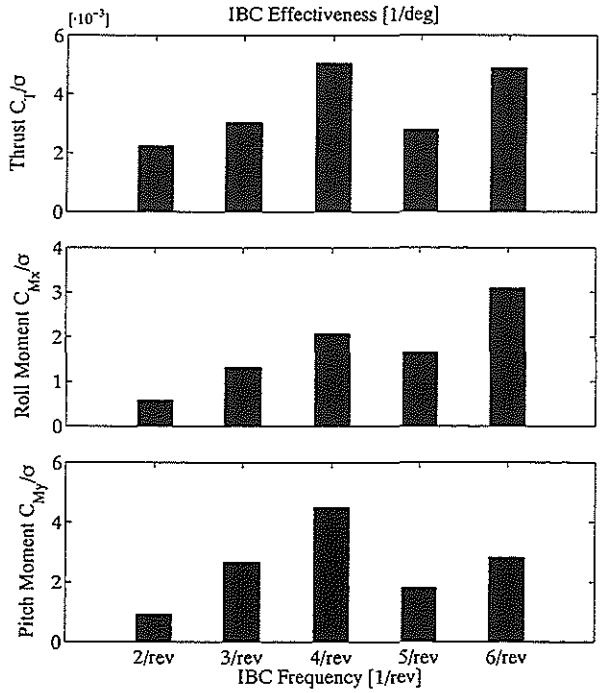

Figure 8: IBC Effectiveness on Thrust C_T/σ, Roll C_{Mx}/σ and Pitch Moment C_{My}/σ Coefficients Derived from BO-105 Rotor Wind Tunnel Data

5.2 Theoretical Explanations

As can be seen from Figure 4 there is no direct path between the 2/rev aerodynamic effects in the rotating frame to the resultant vibrations in the non-rotating frame. As we know, only (N-1)/rev, N/rev and (N+1)/rev blade forces contribute to the N/rev vibrations in the fuselage, whereas the remaining components cancel each other due to the rotor symmetry. This property holds as long as all blades are perfectly identical. Otherwise, residual vibrations of frequencies other than N/rev will additionally occur in the non-rotating frame. However, practical experience shows that for fairly well balanced and tracked blades these vibrations are of much smaller amplitude than those with blade-harmonic frequencies. Therefore, for the following discussions all blades are assumed to be identical. Moreover, all examples refer to a four-bladed rotor as obviously do all BO-105 test results.

The question left to be answered is, which mechanisms of inter-harmonic coupling exist in the rotating frame that link 2/rev IBC inputs to frequencies that finally make their way down to the fuselage.

5.2.1 Simplified Rotor Model

To answer the above question, a very simple rotor model was used for some theoretical investigations. The model only represents the first rigid flapping mode for each blade. Lead-lag motion as well as elastic bending modes of higher order are neglected. For small variations about a given rotor operating condition the following periodically time-variant linear differential equation was derived, which describes the flapping motion of an isolated blade.

$$\beta'' + \gamma D(\psi)\beta' + \left[\gamma K(\psi) + K_0\right]\beta = \gamma\left[E_1(\psi)\vartheta_1 + E_2(\psi)\vartheta_{root} + E_3(\psi)\delta\right]$$

The coefficients D, K and E which depend on the blade properties and the advance ratio can be found in Ref. [14]. In order to relate the flapping motion to those vibratory blade loads which finally propagate to the non-rotating frame, the vertical blade root shear force Z_s was considered a representative parameter. This blade root shear force directly depends on the state variables of the flapping equation and is given by

$$\frac{Z_s}{\Omega^2 S_\beta} = \beta'' + \gamma G(\psi)\beta' + \gamma H(\psi)\beta - \gamma\left[Q_1(\psi)\vartheta_1 + Q_2(\psi)\vartheta_{root} + Q_3(\psi)\delta\right]$$

5.2.2 Interharmonic Coupling of Periodic (Parameter Excited) Systems

It is well known that differential equations with periodic coefficients, even when linear from their structure, show certain behavioral similarities to nonlinear systems. The properties considered here concern the forced solution.

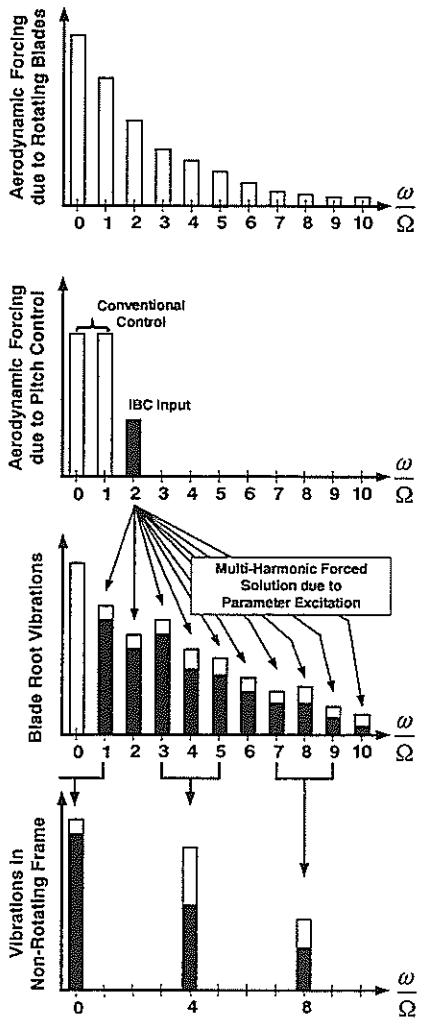

Figure 9: Application of 2/rev IBC to Reduce Vibrations, Effect of Inter-Harmonic Coupling due to Parameter Excitation (4-Bladed Rotor)

While linear time-invariant systems respond to any excitation only with the forcing frequency, the forced solution of periodic systems may contain other frequencies as well. In case of the flapping equation, where the forcing frequencies correspond to integer multiples of the basic period (i.e. the rotor frequency), the forced solution is composed of all integer multiples of the rotor frequency. Thus, even a single-harmonic 2/rev forcing function will produce a multi-harmonic system response containing all components 0/rev, 1/rev, 2/rev, 3/rev,... A more detailed description of the behavior of periodic systems can be found in Refs. [21] or [22].

In addition, any periodical input variable combined with the periodical character of the right hand side coefficients, which are given below for the approximation $a/R = 0$, leads to products of sine and cosine terms in the forcing function.

$$G(\psi) = \frac{1}{9} + \frac{1}{6}\mu\sin(\psi)$$

$$H(\psi) = \frac{1}{6}\mu\sin(\psi) + \frac{1}{3}\mu^2\cos(\psi)\sin(\psi)$$

$$Q_1(\psi) = \frac{1}{12} + \frac{2}{9}\mu\sin(\psi) + \frac{1}{6}\mu^2\sin^2(\psi)$$

$$Q_2(\psi) = \frac{1}{9} + \frac{1}{3}\mu\sin(\psi) + \frac{1}{3}\mu^2\sin^2(\psi)$$

$$Q_3(\psi) = \frac{1}{6} + \frac{1}{3}\mu\sin(\psi)$$

This in turn yields a multi-harmonic excitation even for single-harmonic control inputs through the usual effect of frequency splitting by $\pm\Omega$. Figure 9 summarizes the consequence of these mechanisms for the application of 2/rev IBC to reduce vibrations.

To give an impression of the quantitative relations, some simulations have been evaluated with respect to the spectra of β and Z_s provoked by 1/rev and 2/rev control inputs. The results are shown in Figure 10 and based on the two different configurations defined in Table 1. The cases A and B refer to an idealized rotor at $\mu = 0.5$ with all right hand side input parameters except the single harmonic pitch input set to zero. Both 1/rev and 2/rev inputs provoke response frequencies other than the exciting ones. The cases C and D reflect a more realistic condition at $\mu = 0.35$, where the rotor is loaded and the conventional 1/rev control is used to suppress the 1/rev flapping motion. Again, frequencies such as 3/rev and 4/rev are clearly affected by the 2/rev input. It is hardly necessary to mention that the described inter-harmonic coupling diminishes if the forward speed is reduced to smaller values. At $\mu = 0.1$ the effect has vanished almost completely.

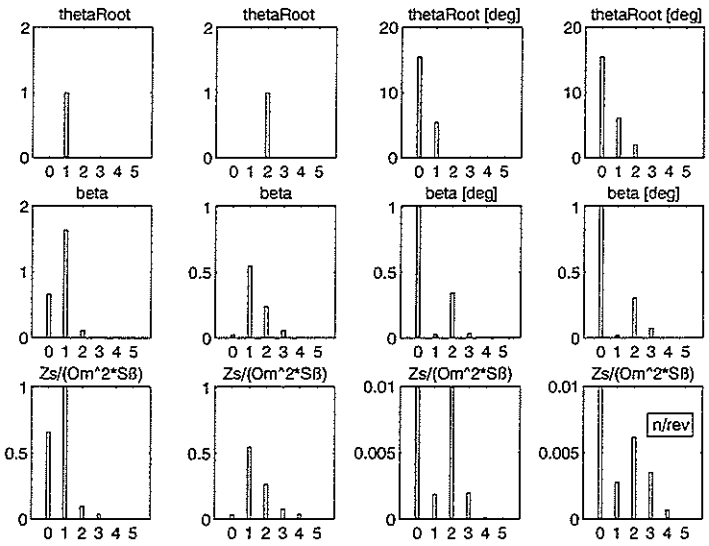

Figure 10: Multi-Harmonic Response (β and Z_s) to Single-Harmonic Forcing Function (A_0, A_1 and A_2) in Presence of Parameter Excitation (for Details See Table 1)

Case	A	B	C	D
Fig. 10	far left	mid left	mid right	far right
A_1	1rad	0	5.4deg	6.1deg
A_2	0	1rad	0	2.0deg
μ	0.5		0.35	
δ	0		-0.065	
ϑ_{Twist}	0		-8deg	
$\vartheta_{0\ root}$	0		15.5deg	
Blade Model	idealized unloaded rotor		≈ BO-105 level flight (re-trimmed for zero 1/rev flapping)	
γ	8			
a/R	0			

Table 1: Parameters Used for the Simulations Presented in Figure 10

5.2.3 Multi-Harmonic Blade Response due to Impulsive Forcing

Another attempt to describe the mechanism of inter-harmonic coupling relies on the idea of impulsive excitation. This description implies that a linear system which is excited through an impulsive but periodic input responds in multi-harmonic frequencies. Applied to the rotor this means that the blades excited by an impulsive disturbance respond with multi-harmonic oscillations. They in turn lead to the undesired vibrations in the non-rotating frame. If 2/rev control was able to affect the disturbance in some way, this input would subsequently have an indirect feed-through onto the vibratory loads in the non-rotating frame (Figure 11).

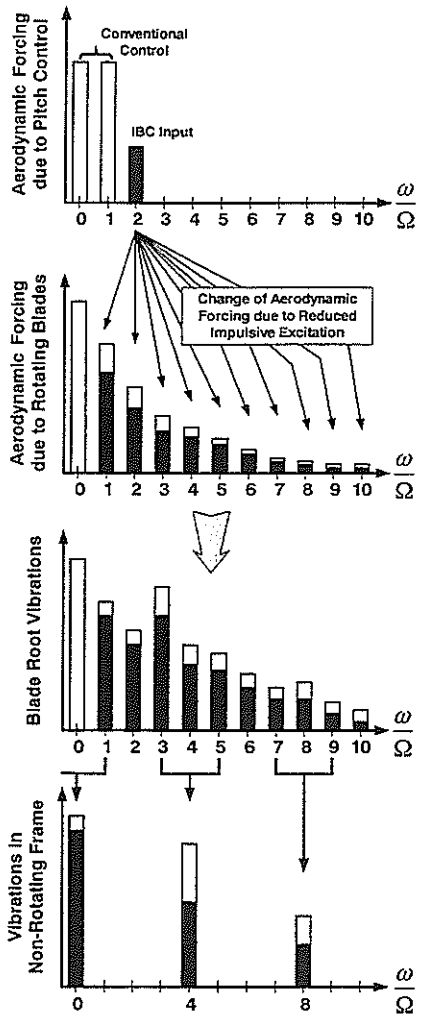

Figure 11: Application of 2/rev IBC to Reduce Vibrations, Effect of Avoiding Inpulsive Excitations in Order to Reduce Multi-Harmonic Forcing

Modeling the Rotor Blade Response to Impulsive Excitation

To investigate the above mentioned mechanism the simple rotor model of chapter 5.2.1 was used again. In contrast to the theoretical investigations there, now only hover i.e. $\mu = 0$ needed to be considered.

This yields to constant coefficients in the above ODE. Now, all four blades were actually modeled and simulated in parallel. The vibrations in the non-rotating frame were then calculated by applying the following summations and transformations to the individual blade components

$$T = -\sum_{i=1}^{N} Z_i \ , \ M_x = a\sum_{i=1}^{N} Z_i \sin\psi_i \ , \ M_y = a\sum_{i=1}^{N} Z_i \cos\psi_i \ .$$

The block diagram of Figure 13 gives an overview of the complete model used to investigate the effect of impulsive disturbances. The two input variables relevant for the following discussion are blade pitch and inflow angle. Their impact on the vertical blade root shear force is shown in the BODE plots of Figure 12.

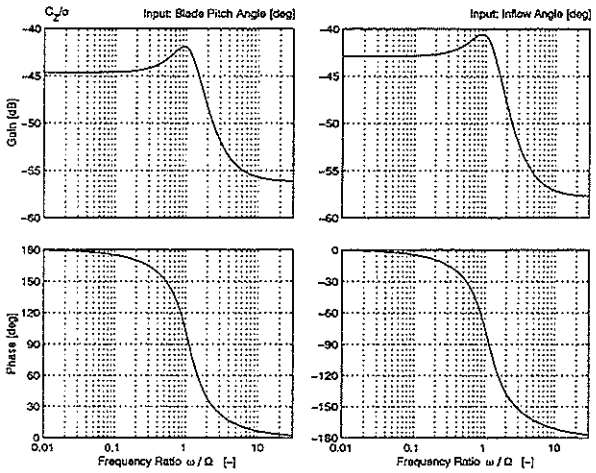

Figure 12: BODE Plot of Vertical Blade Root Shear Force due to Blade Pitch Input (Left) and Inflow Angle (Right)

The non-constant portion of the inflow was assumed to consist of discrete impulsive peaks of initially constant magnitude. In the presented example, two unequally spaced peaks were positioned over one rotor revolution. Figure 14 shows how in the reference case blade flapping responds to the impulsive inflow disturbances.

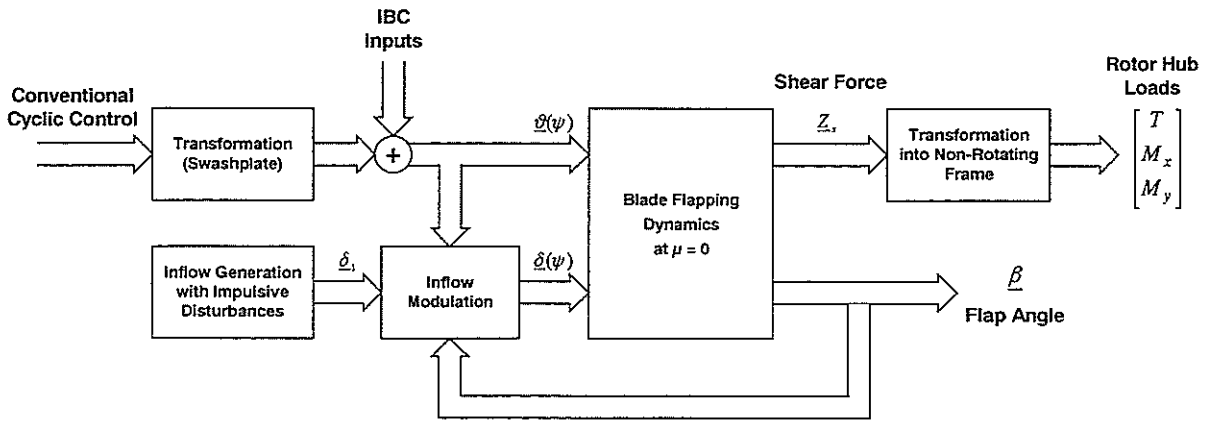

Figure 13: Block Diagram of Simulation Model Set Up to Investigate the Effect of Impulsive Inflow disturbances on Vibration Reduction Mechanism

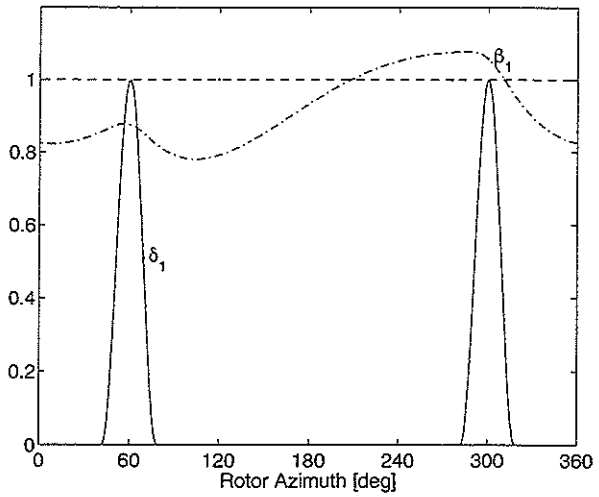

Figure 14: Assumed Inflow Peak Time History and Resulting Flap Angle Response (Reference Case without Inflow Modulation)

This type of impulsive but periodic excitation obviously causes a blade response that contains all frequencies $n\Omega$, which in turn produces the undesired vibrations in the fuselage as discussed before, compare Figure 15. The harmonic contents of the blade response gets richer, when the pulses are shortened in relation to the rotor revolution.

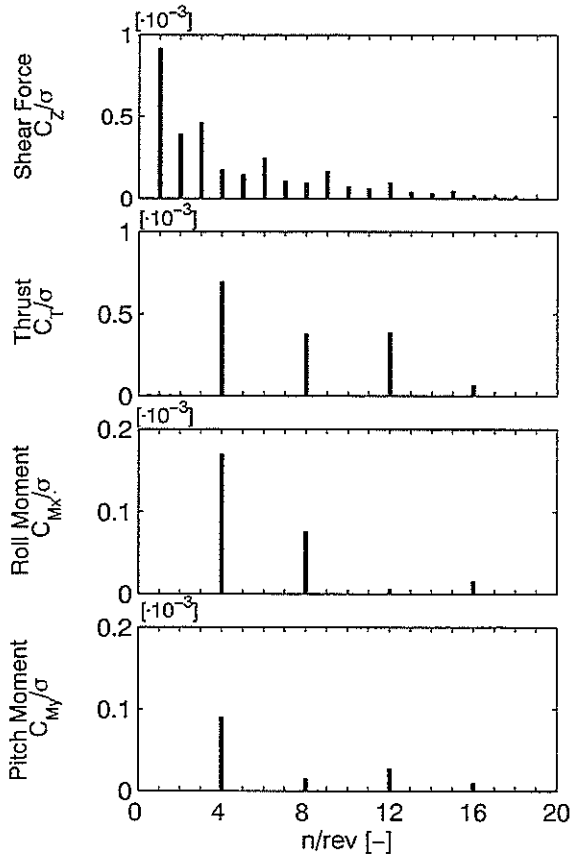

Figure 15: Spectra of Vertical Blade Root Shear Force (Top) and Thrust, Roll, Pitch Moment in the Non-Rotating Frame due to Impulsive Inflow Disturbances (Upper-Mid to Bottom)

One may think of these disturbances as being caused in some sophisticated manner by blade vortices or blade tailboom interference. It has to be stressed that the model was intended to capture only the basic effect and is of course not capable to provide any meaningful prediction.

The simple key idea is now that IBC and not least its 2/rev component directly or indirectly can influence the inflow disturbance strength. This is represented by the block "Inflow Modulation" in Figure 13. Since it was intended to show the principle mechanism only, a simple multiplication was chosen for this block. By no means it was attempted to model any realistic physical mechanism as for example the modulation of the blade vortex strength or the changing of the blade/vortex miss distance through blade pitch control.

Simulation Results

To demonstrate the 2/rev effect of IBC, two cases were investigated. First, the inflow peak intensity at a fixed rotor azimuth angle was assumed to be a direct function of the local blade pitch angle and second a function of the local flap angle. By properly tuning the 2/rev control phase angle, the inflow peaks could be attenuated and as a consequence the vibrations in the non-rotating frame. Figure 16 shows simulation results for various 2/rev control phase angles using the inflow modulation by ϑ. The ellipsoid graphs clearly show the expected influence of 2/rev control. This second explanation of the 2/rev influence seems to be an ideal complement to the first one, because it does not require those high advance ratios to become effective.

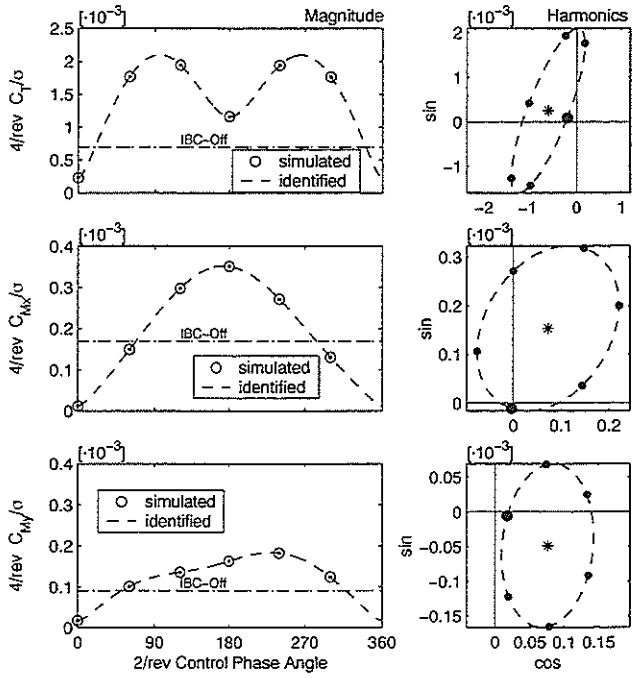

Figure 16: 4/rev Hub Loads in the Non-Rotating System vs. IBC Phase Angle for Single-Harmonic 2/rev control, A_2 = 2deg (δ Modulated by ϑ)

6. Effect of IBC on Pitch Link Loads

Beside the diminishing power efficiency of the rotor some other adverse effects put an upper limit on the maximum forward speed. One of these problems usually encountered at high speed concerns high pitch link loads. Note that the pitch link loads are taken representative for undesired high loads in the complete control chain, which may include much weaker elements than the push rods themselves. Figure 17 gives an impression of the harmonic contents of the pitch link loads as measured for the BO-105 rotor during the full-scale wind tunnel tests mentioned above. This picture shows clearly that the 2/rev components substantially contribute to the control force.

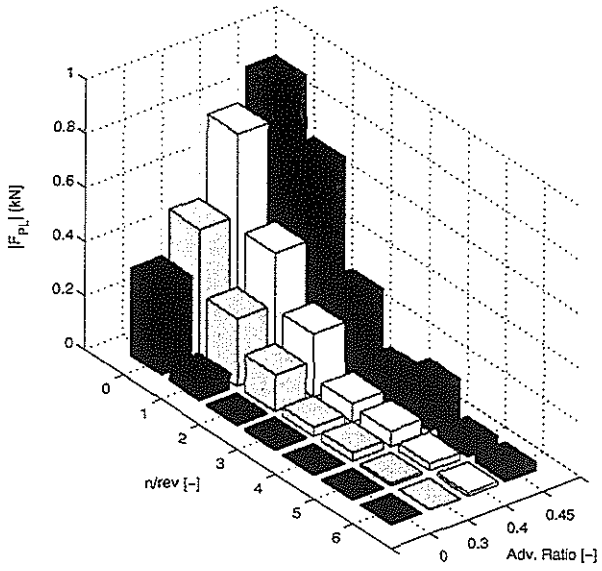

Figure 17: Harmonic Components of Pitch Link Load at Different Advance Ratios (Wind Tunnel Results with Full-Scale BO-105 Rotor)

As one would expect, introduction of 2/rev actuator motions in the rotating frame primarily changes the 2/rev component of the pitch link load. All secondary effects on adjacent harmonic components stay below approximately 30% of the 2/rev effectiveness.

Figure 18 shows how effective 2/rev control can be used to suppress the 2/rev component of the pitch link load. The presented example corresponds to an IBC amplitude of A_2 = 1deg with the best phase out of the 30deg increments investigated during that experiment. In this particular case, the change in the conventional 1/rev control necessary to re-trim the rotor had an additional positive effect on the 1/rev component.

The last set of diagrams in Figure 19 shows how favorable the influence of 2/rev can turn out. As can be seen from the upper two diagrams, the chosen amplitude of 1deg has almost exactly matched the optimal value, while the phase could have been adjusted slightly better for perfect suppression of the 2/rev force component. It should be noticed here that the nonlinear *T*-matrix approach again proves well suited to represent the recorded data.

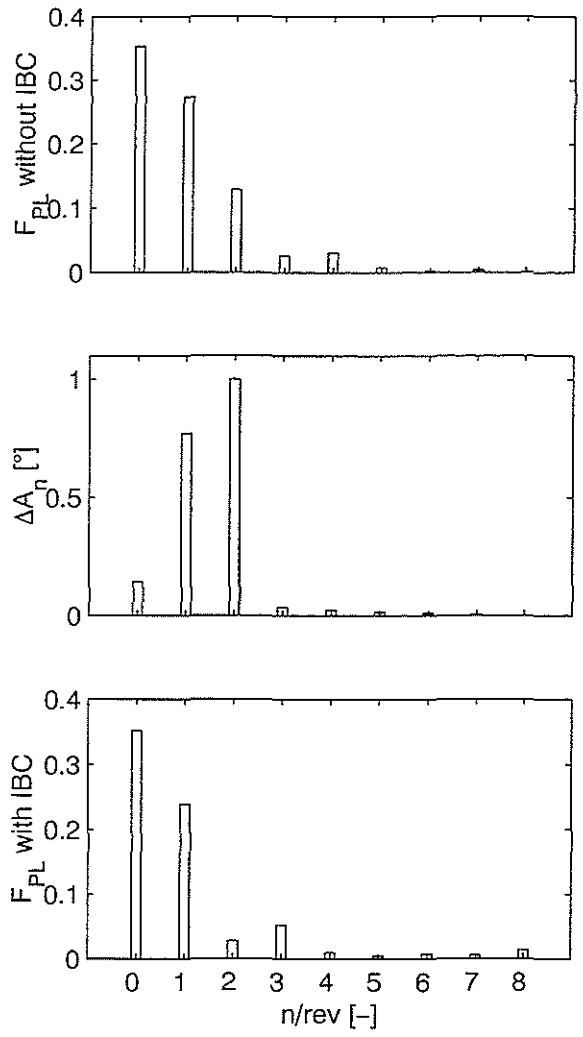

Figure 18: Change of Pitch Link Load Spectrum due to Single Harmonic 2/rev Control, A_2 = 1deg, φ_2 = 280deg (Wind Tunnel Results with Full-Scale BO-105 Rotor)

The time history given in the lower diagram, finally shows the optimum 2/rev control with respect to the peak-to-peak values. By slightly shifting the control phase it is possible to further fine-tune the amplitude and phase relations between the affected harmonic components. This improves the reduction of the peak-to-peak value from about 22% for the case with optimum 2/rev suppression Figure 18, to about 32%.

The application of higher frequencies becomes increasingly ineffective, because the positive effects from reducing the aerodynamic blade pitch moment is compensated by growing inertial moments.

It is worthwhile mentioning that for 2/rev control there exist control phases for which the averaged mechanical power to be provided by the IBC actuator to drive the blade becomes negative, see Ref. [15]. In these cases the phase relation between the controlled actuator motion and the resultant force is such that over one rotor revolution mechanical energy is exchanged but not dissipated.

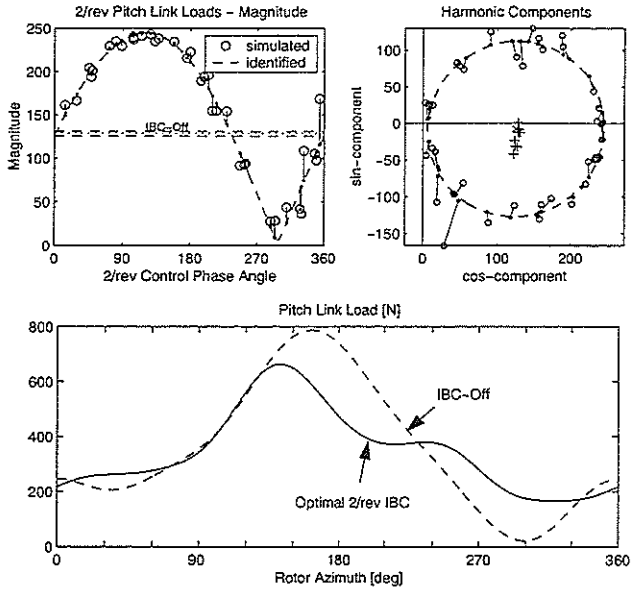

Figure 19: 2/rev Pitch Link Load Component vs. IBC Phase Angle φ_2 for Single-Harmonic 2/rev Control (Upper Diagrams) and Time History for Optimum 2/rev IBC, A_2 = 1deg, φ_2 = 340deg (Lower Diagram, Wind Tunnel Results with Full-Scale BO-105 Rotor)

From the recorded data it was found that the optimum control phases for this effect happen to match the control phases for minimum rotor power required. This would suggest that even passive systems might be considered for this particular application not discussed any further here.

7. Conclusions

In order to show the value of 2/rev harmonic control, various results from flight and wind tunnel tests have been presented. In addition, simple analytical models were used to support the conclusions drawn from the evaluated data. An extended non-linear $\underline{T}$-matrix formalism has proven useful in identifying and modeling the relation between 2/rev blade pitch inputs and the resultant 4/rev fuselage vibrations.

As far as vibrations are concerned, the effectiveness of 2/rev is indeed significantly smaller than it is for the HHC frequencies (N-1)/rev, N/rev and (N+1)/rev but it is still sufficiently high to be worthwhile considering.

Furthermore, inclusion of 2/rev as additional control frequency not only adds two more control inputs to the MIMO system but also offers a better chance to avoid negative side effects on secondary cost function parameters. It was shown, for example, that the optimization goals noise and vibration do not collide in the case of (even single-harmonic) 2/rev control. This is in sharp contrast to the observations made earlier during wind tunnel tests of HHC systems, see Ref. [23]. It is, however, quite clear that not all discussed improvements can be achieved simultaneously i.e. with one single set of control amplitudes and phases. On the other hand, applications like the reduction of control system loads will be of interest only during short periods of time, for example when during maneuver flight certain fatigue stress limits are about to be exceeded, which in turn would eat up precious component lifetime.

During the whole BO-105S1 flight test campaign none of the pilots has reported any noticeable impact of 2/rev control on the helicopter trim or handling qualities. Therefore, 2/rev is believed to be a valuable supplement to the classical HHC frequencies not only with respect to rotor power efficiency issues but also for the important optimization goals noise, vibration and pitch link load reduction.

Since the technical realization of 2/rev generally requires a system like IBC which is capable of controlling each blade individually, additional applications become feasible without any extra hardware. Examples are beside others automatic blade tracking, lag damping augmentation, artificial δ_3 or blade load alleviation, see [24]and [25].

8. References

[1] R. Kube, **Effects of Blade Elasticity on Open and Closed Loop Higher Harmonic Control of a Hingeless Helicopter Rotor,** DLR-FB-97-26, Deutsches Zentrum für Luft- und Raumfahrttechnik (DLR), Institut für Flugmechanik, Braunschweig, 1997 (in German)

[2] Yu, Gmelin, Heller, Philippe, Mercker, Preisser, **HHC Aeroacoustics Rotor Test at the DNW - The Joint German/French/US HART Project,** Twentieth European Rotorcraft Forum, Amsterdam, 1994

[3] Splettstoesser, Schultz, Kube, Brooks, Booth, Niesl, Streby, **BVI Impulsive Noise Reduction by Higher Harmonic Pitch Control: Results of a Scaled Model Rotor Experiment in the DNW,** 17th European Rotorcraft Forum, Berlin, 1991

[4] Straub, Byrns, **Application of Higher Harmonic Blade feathering on the OH-6A helicopter for vibration reduction,** NASA contractor report 4031

[5] Wood, Powers, Cline, Hammond, **On Developing and Flight Testing a Higher Harmonic Control System,** 39th Annual Forum of the American Helicopter Society, St. Louis, 1983

[6] W. Miao, S.B.R. Kottapalli, H.M. Frye, **Flight Demonstration of Higher Harmonic Control (HHC) on S-76,** 42nd Forum of the American Helicopter Society, Washington D.C., 1986

[7] Polychroniadis, Achache, **Higher Harmonic Control: Flight Tests of an Experimental System on SA349 Research Gazelle,** 42nd Forum of the American Helicopter Society, Washington D.C., 1986

[8] Shaw , Albion, **Active Control of Rotor Blade Pitch for Vibration reduction: A Wind Tunnel Demonstration,** Vertica, Vol. 4, 1980, pp.3-11

[9] Shaw , Albion, **Active Control of the Helicopter Rotor for Vibration Reduction**, JAHS, Vol. 26, No.3, July 1981, pp. 32-39

[10] Shaw, Albion, Hanker jr., Teal, **Higher Harmonic Control Windtunnel Demonstration of fully effective Vibratory Hub Force Suppression**, 41st Annual Forum of the American Helicopter Society, Fort Worth, TX, 1985

[11] R. Kube, K.-J. Schulz, **Vibration and BVI Noise Reduction by Active Rotor Control: HHC compared to IBC**, 22nd European Rotorcraft Forum, Brighton,1996

[12] D. Morbitzer, U.T.P. Arnold, M. Müller, **Vibration and Noise Reduction through Individual Blade Control,** 24th European Rotorcraft Forum, Marseille, 1998

[13] D. Schimke, U.T.P. Arnold, R. Kube, **Individual Blade Root Control Demonstration – Evaluation of Recent Flight Tests**, 54th Forum of the American Helicopter Society, Washington D.C., 1998

[14] U. Arnold, G. Reichert, **Flap, Lead-Lag and Torsion Stability of Stop-Rotors**, 19th European Rotorcraft Forum, Como, 1993

[15] U.T.P. Arnold, M. Müller, P. Richter, **Theoretical and Experimental Prediction of Individual Blade Control Benefits**, 23rd European Rotorcraft Forum, Dresden, 1997

[16] O. Kunze, U.T.P. Arnold, S. Waaske, **Development and Design of an Individual Blade Control System for the Sikorsky CH-53G Helicopter**, 55th Forum of the American Helicopter Society, Montreal, 1999

[17] P. Richter, A. Blaas, **Full Scale Wind Tunnel Investigation of an Individual Blade Control System for the BO 105 Hingeless Rotor**, 19th European Rotorcraft Forum, Como, 1993

[18] S. A. Jacklin, A. Blaas, S. M. Swanson, D. Teves, **Second Test of a Helicopter Individual Blade Control System in the NASA Ames 40- By 80-Foot Wind Tunnel,** 2nd AHS International Aeromechanics Specialists' Conference, 1995

[19] W. Steward, **Second Harmonic Control on the Helicopter Rotor,** R.A.E. Report Aero. 2472, November 1952

[20] P.R. Payne, **Higher Harmonic Rotor Control - The Possibilities of Third and Higher Harmonic Feathering for Delaying the Stall Limit in Helicopters,** Aircraft Engineering, August 1958

[21] G.H. Gaonkar, D.S. Simha Prasad, D. Sastry, **On Computing Floquet Transition Matrices of Rotorcraft,** Journal of the American Helicopter Society 3/1981

[22] U. Arnold, **Investigations on the Aero-Mechanical Stability of Stop-Rotors** (in German), Doctoral Dissertation, ZLR-Forschungsbericht 94-03, Technical University of Braunschweig, 1994

[23] R. Kube, K.-J. Schultz, **Vibration and BVI Noise Reduction by Active Rotor Control: HHC compared to IBC**, 22nd European Rotorcraft Forum, Brighton, 1996

[24] G. Reichert, U. Arnold, **Active Control of Helicopter Ground d Air Resonance**, 16th European Rotorcraft Forum, Glasgow, 1990

[25] N.D. Ham, **Helicopter Individual-Blade-Control Research at MIT** 1977-1985, Vertica 1-2, 1987

[26] R. Kube, **Effects of Blade Elasticity on Open and Closed Loop Higher Harmonic Control of a Hingeless Helicopter Rotor** (in German), DLR-Forschungsbericht 97-26, 1997